Heme-Binding Characteristics of the Isolated PAS-A Domain of Mouse Per2, a Transcriptional Regulatory Factor Associated with Circadian Rhythms[†]

Kenichi Kitanishi,[‡] Jotaro Igarashi,[‡] Koya Hayasaka,[‡] Naoki Hikage,[‡] Islam Saiful,[‡] Seigo Yamauchi,[‡] Takeshi Uchida,[§] Koichiro Ishimori,[§] and Toru Shimizu*[,‡]

Institute of Multidisciplinary Research for Advanced Materials, Tohoku University, Katahira, Sendai 980-8577, Japan, and Department of Chemistry, Hokkaido University, Sapporo 060-0810, Japan

Received December 7, 2007; Revised Manuscript Received March 13, 2008

ABSTRACT: Neuronal PAS protein 2 (NPAS2), a heme-binding transcriptional regulatory factor, is involved in circadian rhythms. Period homologue (Per) is another important transcriptional regulatory factor that binds to cryptochrome (Cry). The resultant Per/Cry heterodimer interacts with the NPAS2/BMAL1 heterodimer to inhibit the transcription of *Per* and *Cry*. Previous cell biology experiments indicate that mouse Per2 (mPer2) is also a heme-binding protein, and heme shuttling between mPer2 and NPAS2 may regulate transcription. In the present study, we show that the isolated PAS-A domain of mPer2 (PAS-A-mPer2) binds the Fe(III) protoporphyrin IX complex (hemin) with a heme:protein stoichiometry of 1:1. Optical absorption and EPR spectroscopic findings suggest that the Fe(III)-bound PAS-A-mPer2 is a six-coordinated low-spin complex with Cys and an unknown axial ligand. A Hg^{2+} binding study supports the theory that Cys is one of the axial ligands for Fe(III)-bound PAS-A-mPer2. The dissociation rate constant of the Fe(III) complex from PAS-A-mPer2 (6.3×10^{-4} s^{-1}) was comparable to that of the heme-regulated inhibitor (HRI), a heme-sensor enzyme (1.5×10^{-3} s^{-1}), but markedly higher than that of metmyoglobin (8.4×10^{-7} s^{-1}). As confirmed by a Soret absorption spectral shift, heme transferred from the holo basic helix−loop−helix PAS-A of NPAS2 to apoPAS-A-mPer2. The Soret CD spectrum of the C215A mutant PAS-A-mPer2 protein was markedly different from that of the wild-type protein. On the basis of the data, we propose that PAS-A-mPer2 is a heme-sensor protein in which Cys215 is the heme axial ligand.

Circadian rhythms coordinate important physiological functions, both in the brain and in peripheral cells (*1–5*). Briefly, transcription of specific genes, such as *Per* and *Cry*, induced by the Clock/BMAL1[1] heterodimer, leads to translation of the corresponding regulatory proteins, Per and Cry, that, in turn, bind to other transcription regulatory proteins, such as the Clock/BMAL1 heterodimer, and inhibit the original transcription. This feedback cycling occurs during the daytime. Specifically, the transcription of *Per* and *Clock* is initiated in the morning, the transcriptional regulatory proteins, Per and Cry, accumulate during the day, and these proteins bind to other regulatory proteins (Clock/BMAL1 heterodimer) in the evening, suppressing transcription overnight.

A heme-bound protein associated with circadian rhythms has been identified (*6–8*). In the forebrain, a heme-bound transcriptional regulatory factor, neuronal PAS protein 2 (NPAS2), binds to BMAL1 instead of Clock, and the NPAS2/BMAL1 heterodimer interacts with the E-box sequence of DNA to activate transcription associated with circadian rhythms. CO gas inhibits transcription induced by the NPAS2/BMAL1 heterodimer, suggesting that NPAS2 is a gas sensor protein, similar to FixL, soluble guanylate cyclase (sGC), CooA, and cystathionine β-synthase (CBS). Experiments performed using the isolated bHLH-PAS-A domain of NPAS2 (bHLH-PAS-A-NPAS2) suggest that heme binding to the PAS-A domain of NPAS2 is essential for interactions with the DNA E-box sequence (*9*). Moreover, Cys and His residues are involved in heme binding to PAS-A of NPAS2 (*10*).

Heme proteins are essential for biological functions. For instance, myoglobin, hemoglobin, cytochrome *c*, and cytochrome P450 are used for the storage and transfer of O_2, electron transfer, and activation of O_2, respectively. Heme

[†] This work was supported in part by Grants-in-Aid from the Ministry of Education, Culture, Sports, Science, and Technology of Japan to T.S.

* Correspondence should be addressed to this author. Tel: +81-22-217-5604, -5605. Fax: +81-22-217-5604, -5605, -5390. E-mail: shimizu@tagen.tohoku.ac.jp.

[‡] Tohoku University.

[§] Hokkaido University.

[1] Abbreviations: NPAS2, neuronal PAS protein 2; Per2, period homologue 2; Cry, cryptochrome; BMAL1, brain and muscle ARNT-like 1; FixL, a heme-binding oxygen sensor kinase; sGC, soluble guanylate cyclase; CooA, a CO-sensing transcriptional factor from the photosynthetic bacterium *Rhodospirillum rubrum*; CBS, cystathionine β-synthase with a heme as a redox and/or CO sensor; *Ec* DOS, heme-regulated phosphodiesterase from *Escherichia coli* toward cyclic-di-GMP with a heme as O_2, NO, and CO sensor; HRI, heme-regulated inhibitor or eukaryotic initiation factor 2α kinase; bHLH-PAS-A-NPAS2, isolated basic helix−loop−helix PAS-A domain of NPAS2; mPer2, mouse Per2; PAS-A-mPer2, isolated PAS-A domain of mPer2; EPR, electron paramagnetic resonance; CD, circular dichroism; Fe(III) complex, hemin or Fe(III) protoporphyrin IX complex; Fe(II) complex, Fe(II) protoporphyrin IX complex; Ni-NTA, Ni^{2+}-nitrilotriacetic acid; SDS−PAGE, sodium dodecyl sulfate−polyacrylamide gel electrophoresis; PVDF, polyvinylidine difluoride.

10.1021/bi7023892 CCC: $40.75
Published on Web 05/15/2008

FIGURE 1: Amino acid sequences of heme-bound PAS proteins, such as the PAS-A domains of *Ec* DOS, NPAS2, mPer2, and *Ec* DOS, and the PAS domain of *Rm*FixL. His77 and His194 are the heme axial ligands for *Ec* DOS and *Rm*FixL, respectively. His119, Cys170, and His171 were assigned as the axial ligands of the Fe(III) hemin complex of NPAS2. Mutated sites (H214, C215, H232, H238, C270, H277, H278, and H316) of mPer2 generated in the present study are underlined. *Rm*FixL is a heme-binding oxygen sensor kinase from *Rhizobium meliloti*.

is additionally used for gas sensing in heme-regulated gas sensor proteins (*11, 12*). FixL, sGC, CooA, and CBS use O_2, NO, and CO gases, respectively, while *Ec* DOS proteins employ all three gases for regulation of their functions. Other types of heme-sensor proteins, termed "heme-responsive heme-regulated proteins", have additionally been identified (*13*). In this group, association and/or dissociation of the heme iron complex *per se* to and/or from the protein regulate(s) their functions. For example, a heme-regulated inhibitor (HRI), eukaryotic initiation factor 2α kinase, is inactive due to blockage of the active site by heme in red cells or reticulocytes (*14*). This enzyme becomes activated due to heme iron dissociation from the active site and release from catalytic blockage when the heme concentration is lowered in blood diseases.

A recent cell biology report suggests that mouse Per2 (mPer2) is also a heme-binding protein and that heme exchange between NPAS2 and mPer2 is critical to regulate transcription associated with circadian rhythms (*15*). The same authors propose that the heme shuttle between NPAS2 and mPer2 acts in concert with heme synthesis and degradation. The amino acid sequences of the PAS-A domains of mPer2 and NPAS2 are similar (18% identity, 58% similarity) (Figure 1). In addition, the PAS domain is important for signal transduction, sensing, protein−protein interactions, and transcription (*16, 17*) and serves as a binding site for flavin, heme, or other molecules to induce intermolecular or interdomain signal transduction (*18–20*). The heme iron complex-bound PAS subdomains play a critical role in gas or redox sensing to facilitate catalytic and DNA binding functions in response to external stimuli (*11, 12, 21, 22*). It is reasonable to assume that the heme iron similarly binds to the PAS-A domain of mPer2 and participates in the regulation of transcription associated with circadian rhythms.

In the present study, we examined the heme-binding ability of the isolated PAS-A domain of mPer2 (PAS-A-mPer2) using optical absorption, electron paramagnetic resonance (EPR), circular dichroism (CD), and resonance Raman spectral spectroscopy. PAS-A-mPer2 displayed the ability to bind both Fe(III) and Fe(II) complexes. It is suggested that the heme axial ligands of Fe(III) in PAS-A-mPer2 are Cys and an unknown ligand forming a six-coordinated low-spin complex. Redox-dependent ligand switching occurs from Cys to another amino acid upon reduction of the heme iron from Fe(III) to Fe(II) complexes. His and Cys residues of mPer2 were mutated on the basis of amino acid sequences and proposed axial ligands of the other homologous heme-binding PAS proteins, NPAS2, *Ec* DOS, and FixL (Figure 1). Spectra of Cys and His mutant proteins suggested that Cys215 is the axial ligand of the Fe(III) complex and hydroxide ion is the potential candidate axial ligand *trans* to Cys215. Rapid heme dissociation from the PAS-A-mPer2 protein and heme shuttling from bHLH-PAS-A-NPAS2 to PAS-A-mPer2 further support the theory that mPer2 is a heme-responsive heme-sensor protein, similar to HRI.

EXPERIMENTAL PROCEDURES

Materials. The mouse brain cDNA library was purchased from Invitrogen (Carlsbad, CA). Oligonucleotides were

synthesized by Nippon Gene Research Laboratories Inc. (Sendai, Japan). Restriction, modification, and other enzymes necessary for PCR were obtained from Takara Bio (Otsu, Japan), Toyobo (Osaka, Japan), New England Biolabs (Beverly, MA), and Roche Diagnostics (Tokyo, Japan). The cloning vector, pBluescript II SK(+), and an expression vector, pET28a(+), were purchased from Stratagene (La Jolla, CA) and Novagen (Darmstadt, Germany), respectively. *Escherichia coli* competent cells, XL1-Blue (for cloning) and BL21(DE3)-CodonPlus RIL (for protein expression), were purchased from Stratagene. Other chemicals of the highest guaranteed grade available were acquired from Wako Pure Chemicals (Osaka, Japan).

Construction of Expression Plasmids of PAS-A of mPer2. To generate a plasmid coding for His_6-tagged PAS-A (residues 1−327) of mPer2, the mouse brain cDNA fragment was amplified by PCR using the following primers: forward primer, 5′-GAG**GTCGACATATG**AATGGATACGTGGACTTC-3′, and reverse primer, 5′-GAC**GAATTC**TTACTCAGGAGGGATTCTAGG-3′. Restriction sites are shown in bold, and the stop codon is underlined. Primers for the 5′ ends contained *Sal*I and *Nde*I, and those for the 3′ ends contained *Eco*RI restriction sites for subcloning. Amplified products were digested with *Sal*I and *Eco*RI and subcloned into the pBluescript II SK(+) cloning vector. The nucleotide sequence was confirmed by sequencing. The vector was digested with *Nde*I and *Eco*RI and the isolated fragment subcloned into pET28a(+), which introduces a His_6 tag and thrombin cleavage site at the N-terminus of the desired protein.

Site-Directed Mutagenesis. To generate PAS-A-mPer2 mutants, the PCR-based QuikChange mutagenesis kit from Stratagene was employed, using pET28a containing wild-type PAS-A as the template. The required mutation was confirmed by sequencing. Oligonucleotides used to amplify mutant PAS-A-mPer2 constructs are listed in Supporting Infomation.

Protein Expression and Purification. Wild-type and mutant proteins were expressed in *E. coli* BL21(DE3)-CodonPlus RIL harboring the pET28a(+) expression vector. Briefly, *E. coli* BL21(DE3)-CodonPlus RIL was transformed with the required plasmid, plated on Luria−Bertani (LB) containing 50 μg/mL kanamycin and 50 μg/mL chloramphenicol, and incubated at 37 °C overnight. The next day, a single colony was inoculated in LB medium containing 50 μg/mL kanamycin and 50 μg/mL chloramphenicol and shaken overnight at 200 rpm and 37 °C. The culture medium was added to terrific broth (TB) (1:1000 dilution) containing 50 μg/mL kanamycin and 50 μg/mL chloramphenicol and shaken at 120 rpm and 37 °C. At an OD_{600} value of 0.6, the medium was cooled to 20 °C, and protein expression was induced by adding 0.1 mM isopropyl β-D-thiogalactopyranoside, followed by further shaking for 20 h. *E. coli* cells were harvested by centrifugation for 10 min at 6000 rpm and 4 °C, frozen in liquid nitrogen, and stored at −80 °C until purification. *E. coli* cells expressing PAS-A-mPer2 were suspended in buffer A (50 mM Tris-HCl, pH 8.0, 100 mM NaCl, 20 mM imidazole, 5 mM 2-mercaptoethanol, 5% glycerol), 1 mM phenylmethanesulfonyl fluoride, 1 μg/mL aprotinin, 1 μg/mL leupeptin, 1 mM EDTA, and 0.2 mg/mL lysozyme. Cells were crushed by pulsed sonication for 2 min (three times with 2 min intervals) on ice using the Ultrasonic Disruptor UD-201 (Tomy Seiko, Tokyo, Japan), and centrifuged at 35000 rpm for 30 min at 4 °C. The supernatant fractions were applied to a Ni-NTA-agarose column (Qiagen, Hilden, Germany). Protein fractions were eluted with a linear gradient of 20−200 mM imidazole in buffer A. Fractions were pooled and dialyzed against 20 mM Tris-HCl, pH 8.0, 100 mM NaCl, and 5% glycerol (buffer B), and then thrombin protease (1 unit/5 mg of protein) was added to cleave the His tag. Subsequently, the sample solution was applied to a Ni-NTA-agarose column, and the His-tag-free protein was eluted in the flow-through fractions using buffer B. The solution containing His-tag-free mPer2 was applied to a DEAE-Toyopearl (Tosoh, Tokyo, Japan) column and eluted with a linear gradient of 100−500 mM NaCl in buffer B. After proteins were dialyzed against 20 mM Tris-HCl, pH 8.0, and 5% glycerol (buffer C), the purified protein was concentrated with an Amicon Ultra device (Millipore, Billerica, MA). Proteins were immediately frozen in liquid nitrogen and stored at −80 °C until use. Concentrations were determined using the Coomassie Brilliant Blue dye binding method for protein (Nacalai Tesque, Kyoto, Japan) and the pyridine hemochromogen method for heme. Purified proteins were >95% homogeneous, as confirmed by SDS−PAGE.

Purification of PAS-A-mPer2 protein using buffer without hemin resulted in a mixture of apo- and a small proportion of hemin-bound proteins. To reconstitute PAS-A-mPer2 with hemin, apoprotein was incubated with hemin at a 1:1.2 molar ratio overnight at 4 °C. To remove excess hemin, the solution was loaded onto a DEAE-Toyopearl column.

Expression and purification of bHLH-PAS-A-NPAS2 were performed essentially as described previously (*9*). However, heme reconstitution was performed after His-tag removal in the present study. Briefly, the His-tag-free purified protein was equilibrated overnight on ice with the stoichiometric quantity of hemin prepared in 0.1 M NaOH. Excess hemin was removed with a PD-10 column (GE Healthcare), eluted solutions were collected, and the protein solution was concentrated. Since the heme-binding character of bHLH-PAS-A-NPAS2 is different from that of PAS-A-mPer2, we used different column chromatographies to obtain optimum samples of the two heme-bound proteins.

Determination of the N-Terminal Sequence. After SDS−PAGE, proteins were electroblotted onto PVDF membranes. The N-terminal sequences of protein bands were determined from Edman degradation by Hokkaido System Science Co. Ltd. (Sapporo, Japan). N-Terminal sequencing of the His-tag-free protein disclosed the presence of Gly-Ser-His-Met-Asn-Gly-Tyr-Val-Asp-Phe. Gly-Ser-His is derived from the pET28a vector, while Met is the first residue of mPer2.

Optical Absorption and CD Spectra. Optical absorption spectral experiments under aerobic conditions were performed on a Shimadzu UV-2500 spectrophotometer maintained at 25 °C. Anaerobic spectral experiments were conducted on a Shimadzu UV-1650 spectrophotometer at 15 °C in an anaerobic glovebox at an O_2 concentration less than 100 ppm (Hirasawa, Tokyo, Japan). To ensure the appropriate solution temperature, the reaction mixture was incubated for 10 min, prior to spectroscopic measurements. CD spectra were obtained with a Jasco J-720 CD spectrometer at room

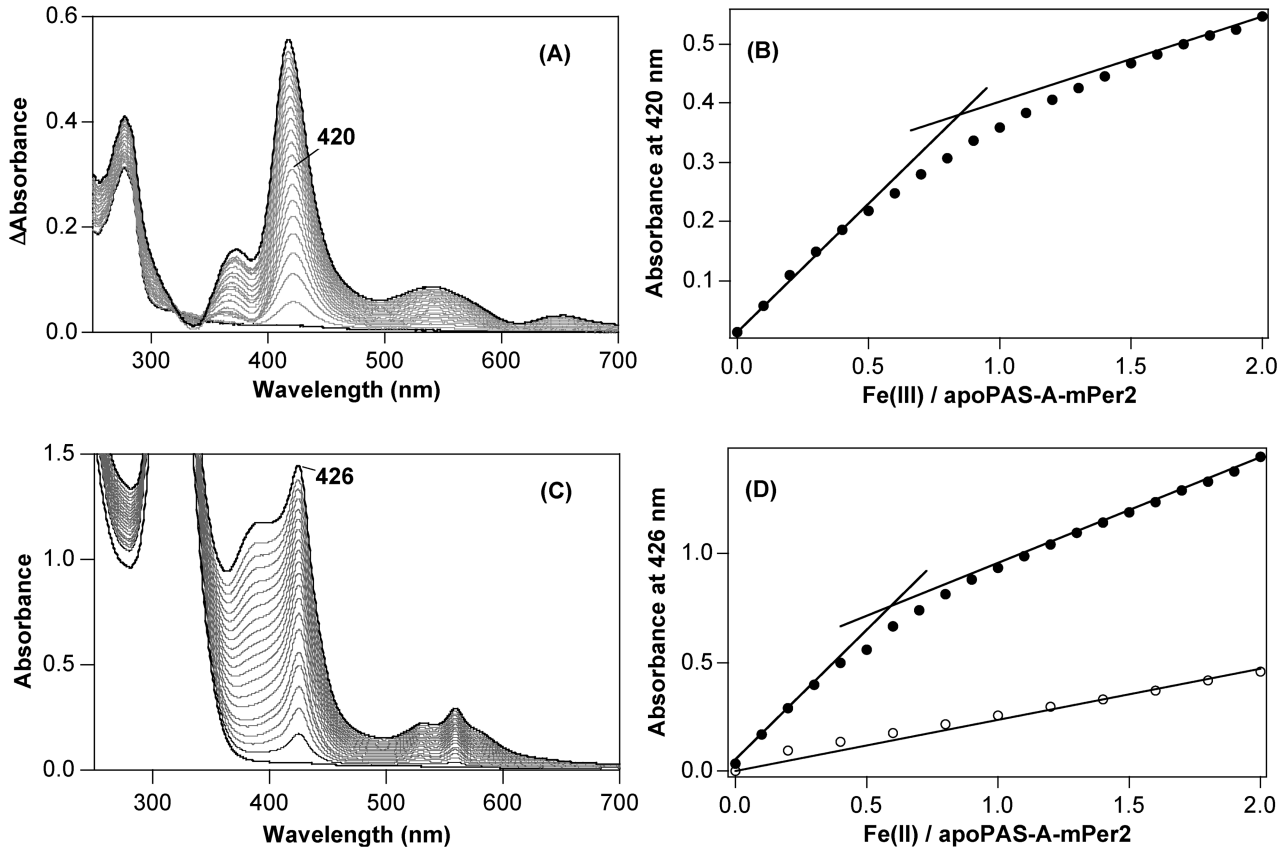

FIGURE 2: Optical absorption spectral changes (left) of PAS-A-mPer2 (10 μM) induced by adding Fe(III) (A) and Fe(II) (C) complexes and intensity changes (right) of spectra monitored at 420 nm for the Fe(III) complex (B) and 426 nm for the Fe(II) complex (D) in 100 mM Tris-HCl, pH 8.0, and 10% glycerol. Open circles represent an increase in absorbance of free Fe(II).

temperature. Ellipticity was normalized to the heme concentration determined using the pyridine hemochromogen assay.

EPR Spectra. Fe(III)-PAS-A-mPer2 complexes (200 μM) were prepared in 10 mM Tris-HCl, pH 8.0, containing 50% glycerol at 25 °C for EPR measurements. EPR spectra were recorded on a JEOL FE-3X spectrometer (Tokyo, Japan) at 30 K. Spectra were accumulated 64 times. The modulation frequency and amplitude were 100 kHz and 1 mT, respectively, whereas microwave frequency and power were 9.1292 GHz and 5 mW, respectively. The magnetic field was calibrated using an NMR gauss meter (Echo Electronics, model EFM-2000), and temperature was controlled with an Oxford ITC4 cryosystem.

Resonance Raman Spectra. Resonance Raman spectra were obtained with a single polychromator (SPEX750M; Jobin Yvon) equipped with a liquid nitrogen-cooled CCD detector (Spec-10:400BLN; Roper Scientific). The excitation wavelength employed was 413.1 nm from a krypton ion laser (BeamLok 2060; Newport Corp. & Spectra Physics Lasers, Mountain View, CA). Laser power at the sample point was adjusted to ~5 mW for air-oxidized and dithionite-reduced forms and 0.1 mW for the CO-bound form to prevent photodissociation of CO. Raman shifts were calibrated with indene, CCl_4, acetone, and an aqueous solution of ferrocyanide. The accuracy of the peak position of well-defined Raman bands was ± 1 cm^{-1}. Protein concentrations for RR experiments were approximately 10−20 μM in 50 mM Tris-HCl, pH 8.0.

Heme-Binding Kinetics. Heme association experiments were performed using an RSP-1000 stopped-flow apparatus (Unisoku, Osaka, Japan). For association of the Fe(II)−CO complex, the buffer containing 50 mM Tris-HCl, pH 8.0, and 50 mM NaCl was purged with nitrogen gas for 30 min and saturated with CO gas. The CO−Fe(II) complex was mixed with the apoprotein at 25 °C. Reactions between the protein and CO−Fe(II) complex were monitored at 406 nm (*23, 24*). For association of the Fe(III) complex, the buffer containing 20 mM Tris-HCl, pH 8.0, was used.

Heme dissociation experiments were conducted on a Shimadzu UV-2500 spectrophotometer maintained at 25 °C with a temperature controller. Dissociation of the Fe(III) complex from Fe(III)-PAS-A-mPer2 was examined as Fe(III)−myoglobin formation by monitoring the increase in absorbance at 412 nm upon mixture of Fe(III)-PAS-A-mPer2 (5 μM) with 10-fold excess H64Y/V68F apomyoglobin (50 μM) in 0.2 M sodium phosphate buffer, pH 7.0, containing 0.6 M sucrose at 25 °C (*23, 24*).

RESULTS

Optical Absorption Spectral Changes Induced by Adding Heme Iron Complexes. To examine whether PAS-A-mPer2 is a heme-binding protein and, if so, the number of bound heme molecules, we examined the spectral changes caused by adding heme iron complexes (Figure 2). Spectral changes for the Fe(III) complex titration experiment (monitored at 420 nm) were composed of two phases, the first phase reflecting heme binding to the apoprotein and the second representing nonspecific binding. From the spectral data, we suggest that a 0.8:1 heme:protein complex is formed for the Fe(III) complex.

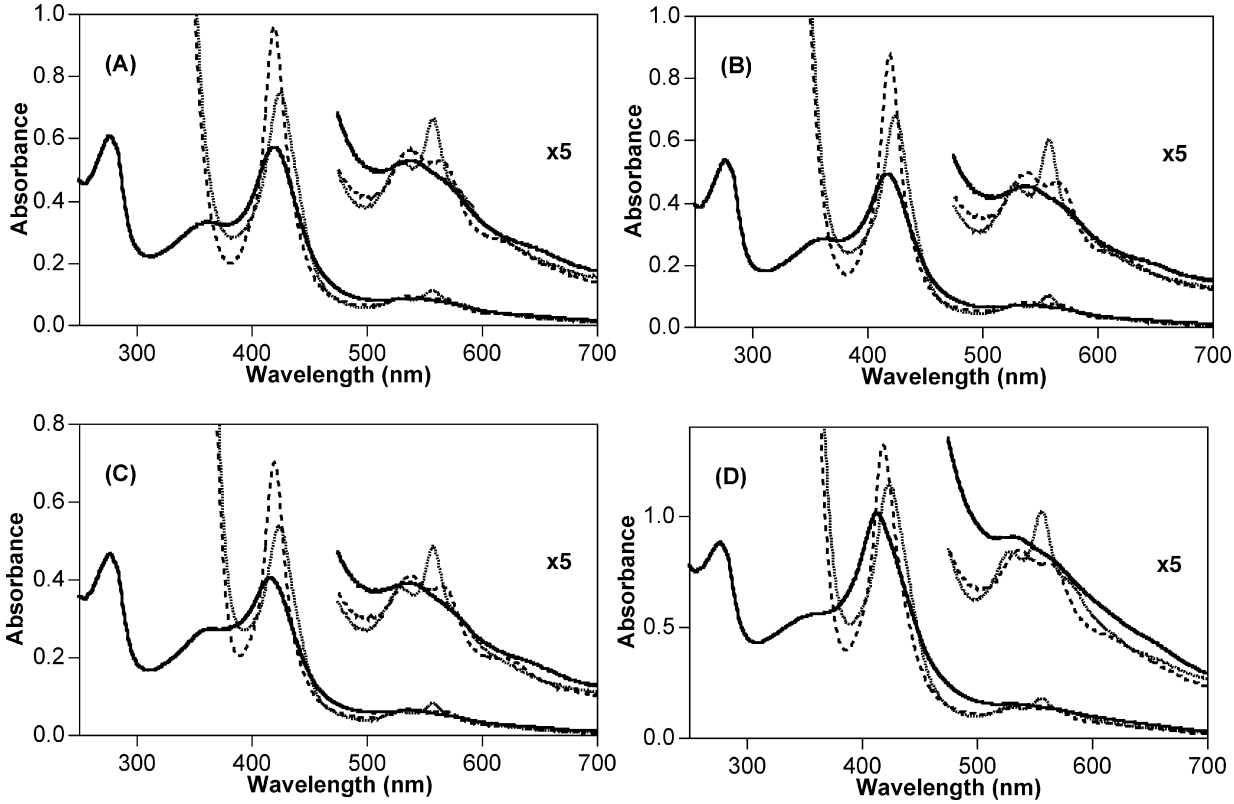

FIGURE 3: Absorption spectra of Fe(III) (solid line), Fe(II) (dotted line), and Fe(II)−CO (broken line) complexes (4 μM) of wild-type (A), C215A (B), H232A (C), and C215A/C270A(D) mutant proteins of PAS-A-mPer2.

Table 1: Optical Absorption Spectra (nm) of PAS-A-mPer2

	Fe(III)		Fe(II)		Fe(II)−CO	
proteins	Soret	visible	Soret	visible	Soret	visible
wild type	421	536	425	529, 558	420	539, 565
H214A	420	539	425	528, 560	421	539, 565
H232A	417	537	426	531, 559	421	537, 568
H238A	419	536	426	529, 560	421	540, 569
H277A	420	539	425	528, 558	420	539, 566
H278A	419	536	425	529, 558	420	539, 564
H316A	421	538	425	530, 558	420	539, 566
C215A	418	537	426	529, 559	421	540, 570
C270A	417	537	426	531, 558	421	539, 561
C215A/C270A	413	531	424	531, 557	419	536, 562

Fe(II) complex binding to the apoprotein was examined under anaerobic conditions. However, a 0.6:1 heme:protein stoichiometry was formed (Figure 2).

Optical Absorption Spectra of Fe(III), Fe(II), and Fe(II)−CO Complexes Bound to PAS-A of mPer2. Optical absorption spectra of the Fe(III), Fe(II), and Fe(II)−CO complexes of wild-type PAS-A-mPer2 are shown in Figure 3A, and spectral peak positions are summarized in Table 1. The Fe(III) complex appears to be a typical six-coordinate low-spin species, based on the spectra reported to date (*25, 26*). The coordination structure is similar to that of the isolated bHLH-PAS-A domain of another heme-bound transcription regulatory factor, NPAS2 (bHLH-PAS-A-NPAS2), where Cys thiolate and His imidazole are the heme axial ligands (*9, 10*). Similarly, spectral changes caused by adding Hg^{2+} and EPR spectral parameters strongly suggest that the Cys thiolate is one of the axial ligands of the Fe(III) hemin complex (Figures 4 and 5). Taking into consideration that Cys thiolate is the axial ligand, the Soret peak at 421 nm of the Fe(III) hemin complex is typical of a S−Fe(III)−N or S−Fe(III)−O complex, as observed for the P450 complexes (*25*). The spectrum of the Fe(III) complex bound to PAS-A-mPer2 was stable and did not alter over a pH range of 7.0−10.0 (data not shown), although precipitates formed below pH 6.0.

The Soret absorption spectral peak of the Fe(II) complex at 425 nm is possibly derived from coordination with a non-thiolate residue distinct from that of Fe(II)−P450 whereby the five-coordinate thiolate-bound complex displays Soret absorption at around 410 nm. The theory that the Fe(II) species of PAS-A-mPer2 has no thiolate coordination is further confirmed by absorption at 420 nm of the Fe(II)−CO complex and resonance Raman spectral results, as discussed below.

Effects of Hg^{2+} on the Optical Absorption Spectrum of the Fe(III) Complex. In case Cys thiolate is the axial ligand of mPer2, as suggested for NPAS2, Hg^{2+} should facilitate the dissociation of heme via interactions with the thiolate anion (*27*). In agreement with this theory, the addition of Hg^{2+} led to an alteration in the Soret band from 421 to 412 nm (Figure 4). Further addition of mercaptoethanol to the Hg^{2+}-containing solution restored the spectral peak to 421 nm, whereas EDTA did not affect the Hg^{2+}-induced absorption band. The 412 nm peak of the Hg^{2+}-containing protein may be attributed to a N−Fe(III)−N or N−Fe(III)−O complex, whereby a new ligand is located near the Cys residue on the protein surface. The thiolate group of mercaptoethanol may partially coordinate to the Fe(III) hemin complex at 421 nm after the addition of excess mercaptoethanol to the Hg^{2+}-containing solution. Thus, results from the Hg^{2+} binding study suggest that one of the axial ligands of the Fe(III) complex of the isolated PAS-A domain of mPer2 is Cys thiolate.

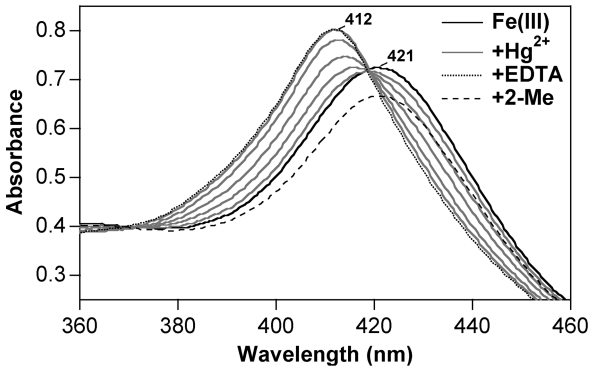

FIGURE 4: Spectral changes of Fe(III)-bound PAS-A-mPer2 induced by adding Hg^{2+}. The Soret band at 421 nm of the protein (4 μM) moved to 412 nm upon the addition of Hg^{2+} (5, 10, 15, 20, and 25 μM). The spectral band at 412 nm was not altered in the presence of EDTA (500 μM). However, the original spectral band due to thiolate coordination was mostly recovered with 2-mercaptoethanol (4 mM).

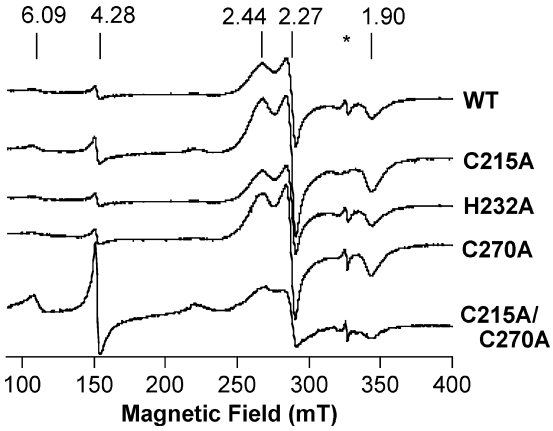

FIGURE 5: EPR spectra of the Fe(III)-PAS-A-mPer2 complex for the wild-type (200 μM), C215A (200 μM), C270A (200 μM), and C215A/C270A (120 μM) mutant proteins in 10 mM Tris-HCl, pH 8.0, and 50% glycerol. The asterisked band represents artifacts.

EPR Spectra of the Fe(III) Complex of PAS-A-mPer2. Crystal field parameters of EPR spectra of Fe(III) low-spin complexes have been successfully used to identify axial ligands of the heme iron (*14, 28*). Thus, we obtained EPR spectra of Fe(III)-PAS-A-mPer2 (Figure 5). The EPR spectrum of Fe(III)-bound PAS-A-mPer2 was characteristic of a low-spin heme complex with *g*-values of 2.44, 2.27, and 1.90 (Figure 5). Crystal field parameters of the PAS-A-mPer2 complex were located in the region for the axial ligands Cys/OH^- but were also close to the Cys/His (bHLH-PAS-A-NPAS2) region (Figure 6) (*36*). Thus, while Cys thiolate is confirmed as the axial ligand, the *trans* Cys ligand for the Fe(III) low-spin complex of PAS-A-mPer2 remains to be established under the present conditions.

Resonance Raman Spectra of the High-Frequency Region. Resonance Raman spectroscopy provides useful information about the heme coordination structure (*10, 12*). In particular, the spin and coordination marker band, ν_3, is essential to understand the coordination number and spin state of Fe(III) complexes (*29*). To elucidate the heme coordination structure, we obtained resonance Raman spectra of Fe(III), Fe(II), and Fe(II)−CO complexes of PAS-A-mPer2. As shown in Figure 7A, the ν_3 band for the Fe(III) complex, observed at 1501 cm^{-1}, was typical of a six-coordinate low-spin complex, in accordance with optical absorption spectroscopy findings.

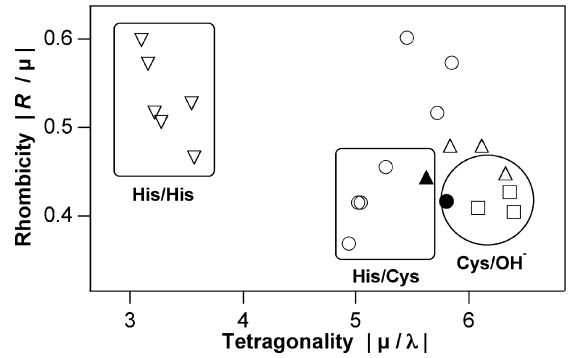

FIGURE 6: Crystal field parameters of PAS-A-mPer2 (●), bHLH-PAS-A-NPAS2 (▲) (*35*), and other selected heme proteins.

The ν_3 band for the Fe(II) complex consisted of two frequencies at 1468 and 1491 cm^{-1}, suggesting the presence of equivalent amounts of both six-coordinate low-spin and five-coordinate high-spin species. The Fe(II)−CO complex contains the same two species as the Fe(II) complex. The five-coordinate high-spin species may be generated from partial photodissociation during measurement (Table 2).

Inverse correlation between the Fe−CO (ν_{Fe-CO}) and FeC−O (ν_{C-O}) stretching frequencies is useful to identify the axial ligand *trans* to CO in the Fe(II)−CO complex. While we examined resonance Raman spectra of the photodissociated five-coordinate Fe(II) heme complex, we collected isotope-sensitive bands in the presence of $^{12}C^{16}O$ (natural) and $^{13}C^{18}O$ gases for the Fe(II)−CO complex of PAS-A-mPer2 (Figure 8). From the difference spectra, bands at 494 and 1964 cm^{-1} were assigned to ν_{Fe-CO} and ν_{C-O} frequencies, respectively. The inverse correlation between the two frequencies indicates that the ligand *trans* to CO is His and not Cys, as observed for the P450 species (Figure 9). The correlation parameter of mPer2 suggested the CO binding environment is apolar and there is no strong electrostatic interaction of CO bound to the Fe(II) complex (*12*).

Association and Dissociation Rate Constants of the Fe(II)−CO and Fe(III) Complexes for PAS-A-mPer2. The heme is proposed to shuttle between mPer2 and NPAS2 to regulate transcription of circadian rhythms. Accordingly, we examined the heme association and dissociation rate constants for PAS-A-mPer2. The association rate constant of the Fe(II)−CO complex for binding to heme-free PAS-A-mPer2 was 3.5×10^7 M^{-1} s^{-1} (Table 3, Figure 10). This value is similar to those of other heme-binding proteins (*9, 23, 24, 28, 30*). The dissociation rate constant of the Fe(III) complex from PAS-A-mPer2 was 6.3×10^{-4} s^{-1} (Table 3, Figure 10), comparable to those of the heme-responsive heme-sensor proteins, HRI and bHLH-PAS-A-NPAS2, but markedly higher than those of sperm whale myoglobin (8.7×10^{-7} s^{-1}) and human hemoglobin α-subunit (7.1×10^{-5} s^{-1}) (*23, 24*) (Table 3). Additionally, the dissociation rate constants of putative heme-transfer proteins, SOUL (6.1×10^{-3} s^{-1}) and p22HBP (4.4×10^{-3} s^{-1}), are very high, equivalent to those of HRI, bHLH-PAS-A-NPAS2, and PAS-A-mPer2, although the intrinsic functions of SOUL and p22HBP are currently unclear (*30*).

We attempted to measure the association rate constant of the Fe(III) complex (hemin) with apoPAS-A-mPer2 by

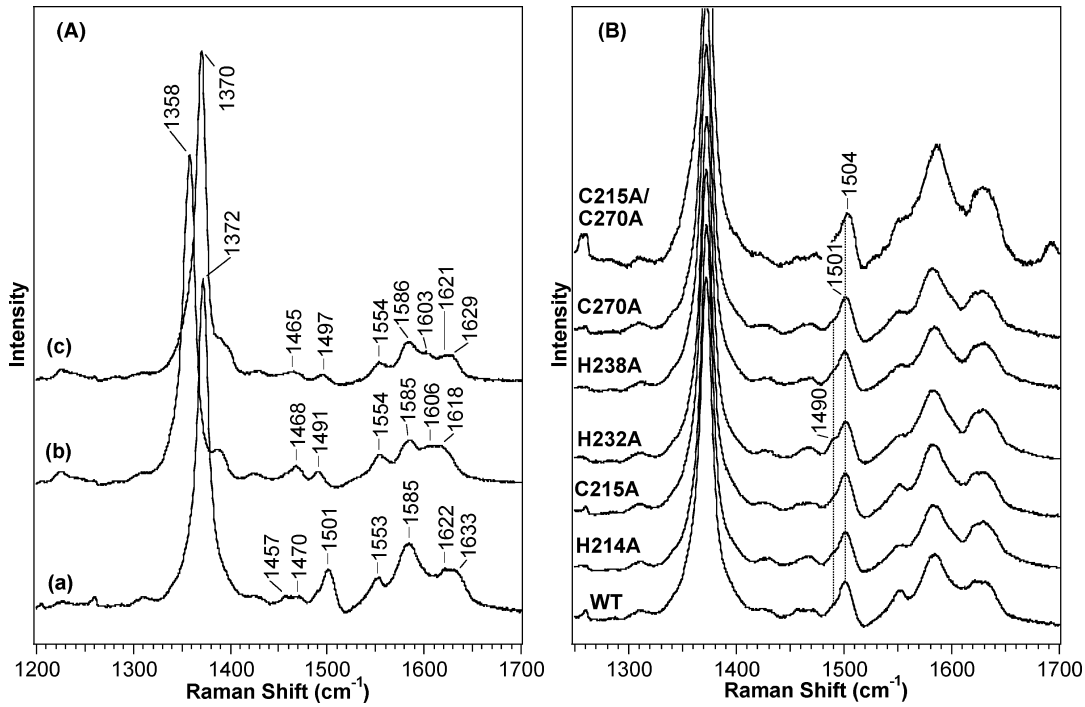

FIGURE 7: Resonance Raman spectra of the high-frequency region of Fe(III) (a), Fe(II) (b), and Fe(II)−CO (c) complexes of wild-type PAS-A-mPer2 (A) and those of selected mutant proteins of Fe(III)-bound PAS-A-mPer2 (B) excited at 413.1 nm.

Table 2: Resonance Raman Spectral Bands of PAS-A-mPer2 (cm^{-1})

	ν_2	ν_3	ν_4	states
Fe(III)	1553, 1585	1457, 1470, 1501	1372	6cLS (major) 5cHS (minor)
Fe(II)	1554, 1585	1468, 1491	1358	6cLS, 5cHS
Fe(II)−CO	1554, 1586	1465, 1497	1370	6cLS, 5cHS

stopped-flow spectrometry, as previously described (*37, 42*). However, we did not observe the protein-concentration dependency of the Fe(III) complex association rate under our experimental conditions (Figure 1S in Supporting Information), in which the Fe(III) complex (hemin) is in equilibrium between monomer (60%) and dimer (40%)

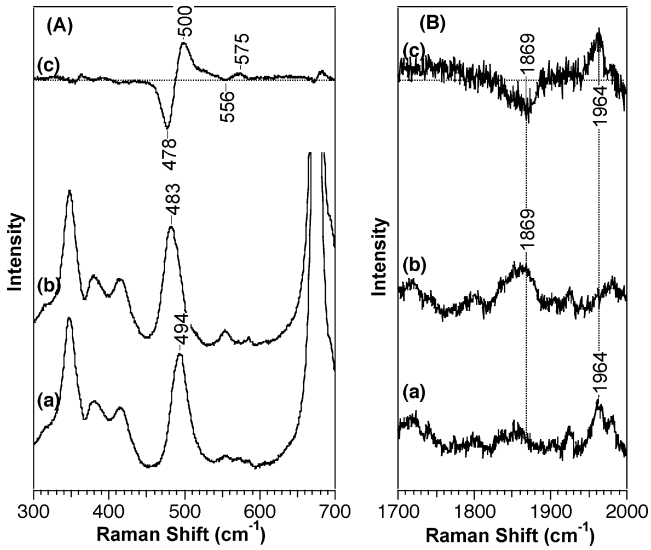

FIGURE 8: Resonance Raman spectra of the Fe(II)−CO complex of PAS-A-mPer2 in the low-frequency (A) and high-frequency (B) regions with excitation at 413.1 nm. Spectra of Fe(II) heme-PAS-A complexes of $^{12}C^{16}O$ (a) and $^{13}C^{18}O$ (b) and the difference ($^{12}C^{16}O$ − $^{13}C^{18}O$) (c).

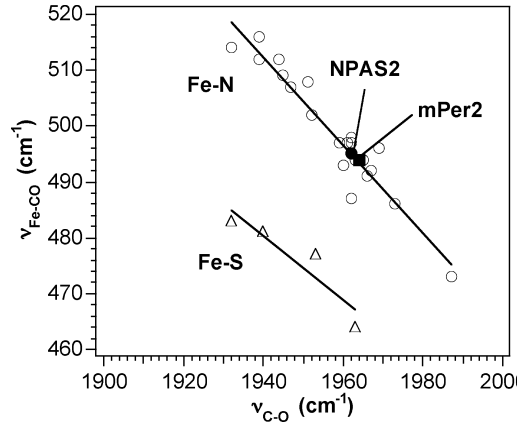

FIGURE 9: Inverse correlation between ν_{Fe-CO} and ν_{C-O} frequencies. Points are denoted with closed circles, and the squares represent bHLH-PAS-A-NPAS2 and PAS-A-mPer2, respectively. Open circles signify various hemoglobins, myoglobins, peroxidases, and proteins containing histidine as their proximal ligand, except BSA that has no specific axial ligand for heme. Parameters located at both ends suggest that there is strong ionic interaction(s) with CO bound to the Fe(II) complex (*12*). Thus, it is suggested for bHLH-PAS-A-NPA2 and PAS-A-mPer2 that there is no such strong electrostatic interaction with CO.

forms (*38, 42*). If the conversion from dimer to monomer is the rate-determining step, it may not be possible to clearly measure a protein-concentration-dependent rate constant.

Transfer of the Fe(III) Complex (Hemin) from NPAS2 to mPer2. It is suggested that heme iron shuttles between NPAS2 and mPer2 to regulate transcription associated with circadian rhythms (*15*). When heme-free bHLH-PAS-A-NPAS2 was added to the Fe(III)-bound PAS-A-mPer2 protein solution, no significant spectral changes were noted (Figure 11A). However, spectral changes were evident upon the addition of heme-free PAS-A-mPer2 to Fe(III)-bound bHLH-PAS-A-NPAS2 (Figure 11B). These spectral changes were slow and limited to 5 min. Nevertheless, it appears that

Table 3: Heme Association and Dissociation Rate Constants for PAS-A-mPer2 and Other Heme-Binding Proteins[a]

protein	k_{on} (M^{-1} s^{-1})	k_{off} (s^{-1})	ref
PAS-A-mPer2	3.5×10^7	6.3×10^{-4}	present work
bHLH-PAS-A-NPAS2	3.3×10^7	5.3×10^{-3}	*9*
HRI	1.1×10^7	1.5×10^{-3}	*28*
SOUL	1.9×10^6	6.1×10^{-3}	*30*
p22HBP	1.0×10^8	4.4×10^{-3}	*30*
Sw Mb[b]	7.6×10^7	8.4×10^{-7}	*23*, *24*
Sw Mb H93G	7.0×10^7	1.2×10^{-2}	*23*, *24*
Hb α-subunit	2.9×10^7	7.1×10^{-6}	*23*, *24*

[a] The association rate constant of the Fe(II)−CO complex and dissociation rate constant of the Fe(III) complex for PAS-A-mPer2 were evaluated assuming that both rates are composed of a single phase. [b] Sw Mb, sperm whale myoglobin.

the Fe(III) complex moves from bHLH-PAS-A-NPAS2 to PAS-A-mPer2 at more than 0.2 min^{-1} under the present conditions.

Fe(III) complex (hemin) transfer kinetics from holobHLH-PAS-A-NPAS2 to apoPAS-A-mPer2 were assessed by stopped-flow spectrometry by monitoring the changes in absorption at 421−422 nm (Figure 2S in Supporting Information) (*37*). However, the Soret absorption peak of holobHLH-PAS-A-NPAS2 at 421 nm overlapped with that of holoPAS-A-mPer2, making it difficult to evaluate the rate of hemin transfer from bHLH-PAS-A-NPAS2 to PAS-A-mPer2 (i.e., decrease of holobHLH-PAS-A-NPAS2 absorption and concomitant increase of holoPAS-A-mPer2 absorption). We found, however, that the rate of the apparent spectral increase partially associated with hemin transfer under these experimental conditions was 1.0×10^{-2} s^{-1}. In agreement with the results obtained by conventional optical absorption spectrometry, we found that the reverse hemin transfer, from holoPAS-A-mPer2 to apobHLH-PAS-A-NPAS2, was not observed by stopped-flow spectrometry.

To further determine whether the transfer of the Fe(III) complex from bHLH-PAS-A-NPAS2 to PAS-A-mPer2 is direct, via protein−protein interaction, or indirect transfer, we performed a pull-down assay. A mixture of holobHLH-PAS-A-NPAS2 and apoHis_6-tagged PAS-A-mPer2 was incubated for 10 min at room temperature and loaded onto a Ni-NTA-agarose column. After the column was washed extensively, the His_6-tagged protein was eluted with the imidazole-containing buffer. SDS−PAGE analysis indicated that bHLH-PAS-A-NPAS2 and PAS-A-mPer2 did not interact directly. However, the absorption spectrum of the Fe(III) complex was associated with PAS-mPer2 solution but not with the bHLH-PAS-A-NPAS2 solution, indicating that bHLH-PAS-A-NPAS2 lost, while PAS-A-mPer2 acquired, the Fe(III) complex, biochemically corroborating the heme transfer from holobHLH-PAS-A-NPAS2 to apoPAS-A-mPer2. In contrast, the reverse transfer reaction of the Fe(III) complex, from holoHis_6-tagged PAS-A-mPer2 to apobHLH-PAS-A-NPAS2, was not observed.

Optical Absorption Spectra of the Fe(III) Complex of Cys and His Mutants of PAS-A-mPer2 Proteins. Since Cys and/or His are (is) the predicted axial ligand(s) of the Fe(III) complex of PAS-A-mPer2, we mutated these residues with a view to identifying the actual axial ligands for the heme iron complex. Heme-bound sites of the PAS-A domain of the companion protein, NPAS2, associated with circadian rhythms, include His119, His171, and Cys170, as observed from resonance Raman spectral studies of the mutant proteins (*10*). The corresponding residues of mPer2 are His 214, Cys 215, and Cys 270 (Figure 1). Accordingly, we mutated these sites as well as additional His residues at 232, 238, 277, 278, and 316. Optical absorption maxima of selected single and double mutant proteins are shown in Figure 3. The wavelengths of all mutant proteins generated are summarized in Table 1. Only three mutant proteins (H232A, C215A, and C270A) displayed slight Soret band shifts (<3 nm), compared with the wild-type protein. Importantly, however, the spectrum of the Fe(III) complex of the C215A/C270A double mutant was significantly different from that of the wild-type protein (Figure 3D) (Table 1).

Dissociation and Association Rate Constants of the Fe(III) Complex for Cys Mutants PAS-A-mPer2. Since our results indicated that Cys215 of PAS-A-mPer2 is the axial ligand for the Fe(III) complex, we measured the dissociation rate constant of the Fe(III) complex from holoC215A of PAS-A-mPer2. We did not observe any significant differences in the dissociation rate constants of the C215A mutant, the C270A mutant, and the wild-type protein. The apparent association rates of the Fe(III) complex to the C215A and C270A mutants were also similar to those of the wild-type protein.

CD Spectra of the Fe(III) Complexes of Cys and His Mutant PAS-A-mPer2 Proteins. The CD spectral band at the Soret region of heme-bound protein reflects subtle structural differences among the heme protein species, and between wild-type and mutant proteins, even if optical absorption bands are not significantly different (*31, 33*). The Soret band of the Fe(III)-bound wild-type PAS-A-mPer2 exhibited a peak at ∼400 nm and a trough at ∼450 nm (black line in Figure 12). The C215A mutant showed a markedly different CD band, specifically, a broad peak with a shoulder at ∼445 nm and a very broad trough from 480 to 500 nm (blue line in Figure 12). The CD spectrum of the C215A/C270A double mutant also showed the CD band substantially different from that of the wild-type protein (green line in Figure 12). In contrast, the CD spectra of H232A, H277A, H278A, and H316A mutant proteins were analogous to that of wild-type protein (Figure 12 and Figure 3S in Supporting Infomation). The H214A, H238A, and C270A mutant proteins displayed different CD spectra from that of wild-type protein, but differences were marginal and not as significant as that of the C215A protein (Figure 4S in Supporting Infomation).

EPR Spectra of Cys and His Mutant Proteins. To identify the axial ligand *trans* to Cys215 and to obtain supporting evidence of Cys215 as the axial ligand, we obtained EPR spectra of selected Cys and His mutant proteins of PAS-A-mPer2. We found that crystal field parameters of His mutant proteins were similar to those of the wild-type protein (Figure 5). Moreover, the EPR spectra and crystal field parameters of the C215A and C270A mutants were similar to those of the wild-type protein (Figure 5). However, the EPR spectrum of the C215A/C270A double mutant was significantly different from those of the wild type and other mutants (Figure 5). For the double mutant, EPR signals due to the five-coordinated high-spin complex ($g = 6.09$) and non-heme iron species ($g = 4.28$) were observed in the lower magnetic field region, whereas the intensity and shape of the EPR spectrum due to the six-coordinated low-spin complex were

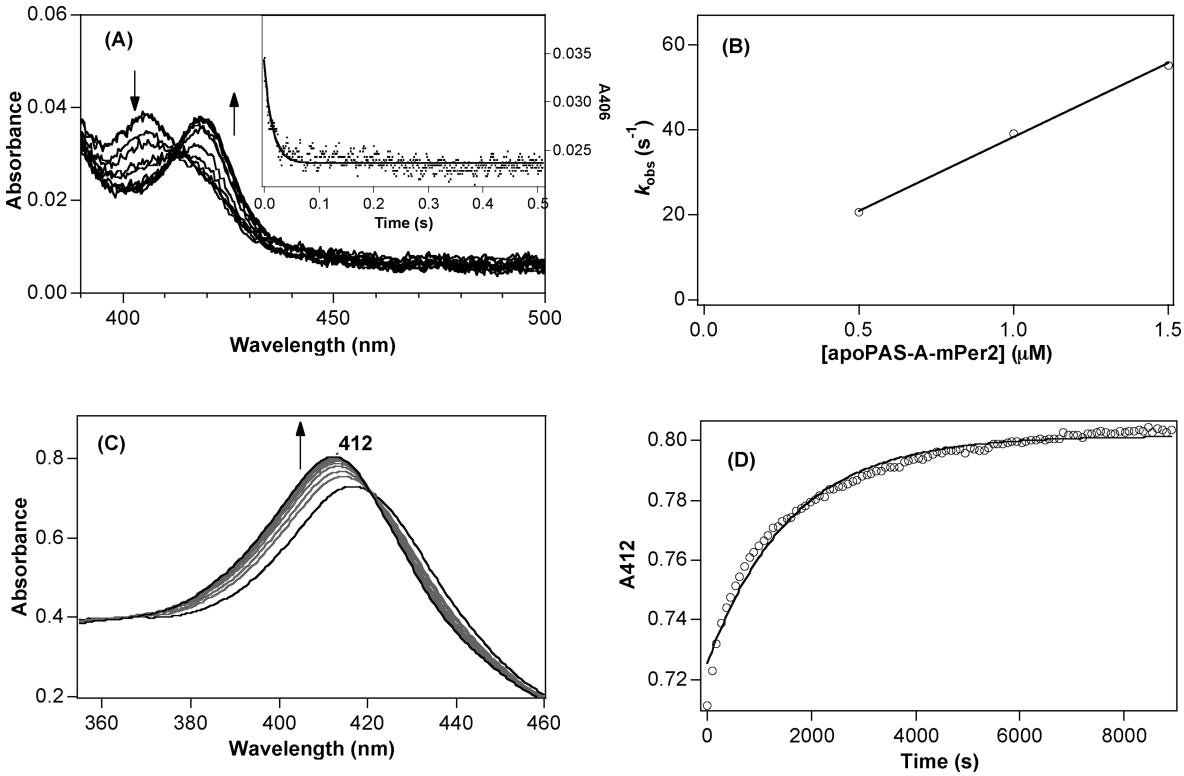

FIGURE 10: Determination of heme association and dissociation rate constants for PAS-A-mPer2. Optical absorption spectral changes accompanying association of the Fe(II)−CO complex (0.5 μM) with heme-free PAS-A-mPer2 (3 μM) (A) after mixing using a stopped-flow spectrometer. The inset depicts spectral changes at 406 nm, composed of only a single phase. Correlation between k_{obs} and the concentration of heme-free PAS-A-mPer2 is shown in (B). Spectral changes accompanying heme dissociation from PAS-A-mPer2 (5 μM) and association to the H64Y/V68F apomyoglobin mutant (50 μM) (C) and upon Fe(III)−myoglobin formation, as monitored at 412 nm with a mixture of Fe(III)-PAS-A-mPer2 and H64Y/V68F apomyoglobin (D). The spectral change was assumed to be composed of a single phase, and the dissociation rate constant (Table 3) was evaluated.

substantially different from those of the wild-type and other mutant proteins.

Resonance Raman Spectra of Mutant Proteins. We obtained resonance Raman spectra of Fe(III) complexes of selected mutant proteins (Figure 7B). Spectra of single mutant proteins were similar to that of the wild-type PAS-A-mPer2 protein, except that of the H232A mutant, whereby a trace amount of the five-coordinate high-spin species was observed. The spectrum of the Fe(III) complex of the C215A/C270A double mutant was that of a typical six-coordinate low-spin species, similar to that of the wild-type protein. However, the ν_3 band (coordination and spin marker band) of the double mutant, at 1504 cm^{-1}, was different from that of the wild-type protein, at 1501 cm^{-1}, suggesting that the double mutant forms a different kind of low-spin complex.

DISCUSSION

A number of heme-responsive heme-sensor proteins have been identified in recent years. Association/dissociation of the heme iron complex to/from heme-sensor proteins regulates catalysis or transcription (*13*). Regulation may be mediated by protein−protein interactions or structural changes induced by heme association/dissociation. Interestingly, heme-responsive heme-sensor proteins, such as HRI, Bach1, IRP2, E75, DGCR8, and the Slo BK channel, contain Cys as the axial ligand at the heme binding site (*13*). Redox-dependent ligand switching from Cys to a residue other than the thiolate of Cys upon reduction of Fe(III) hemin to Fe(II) heme is also characteristic of the heme-responsive heme-sensor proteins (*13*). The heme dissociation rate constant from HRI is three orders of magnitude greater than that from metmyoglobin, implying that labile heme binding to the heme-sensor protein is required to facilitate heme shuttle between this protein and the aqueous complex or other heme-sensor proteins.

The Soret bands of all Fe(III) complexes with Cys as an axial ligand should be similar to that of P450 (*25, 26*). However, five-coordinate thiolate-ligand high-spin Fe(III) complexes of all heme-sensor proteins display Soret absorption around 370 nm, whereas similar complexes of P450 exhibit peaks at around 390 nm (*13, 28, 32*). In the present study, the Cys coordination to PAS-A-mPer2 was proved by the Hg^{2+} titration and EPR spectrum (Figures 4 and 5). However, only the low-spin complex was observed for PAS-A-mPer2, and spectral features were similar to the corresponding P450 complexes with S−Fe(III)−N or S−Fe(III)−O axial ligands. For Fe(III) P450, the S−Fe(III)−N complexes display Soret bands between 421 and 425 nm, whereas S−Fe(III)−O complexes contain bands between 416 and 420 nm. Therefore, the absorption peak at 421 nm of PAS-A-mPer2 is within the boundary region between the S−Fe(III)−N and S−Fe(III)−O complexes. The EPR crystal field parameter of PAS-A-mPer2, located in the S−Fe(III)−O region, is also close to the S−Fe(III)−N region. However, since all His mutant proteins displayed similar optical absorption, CD, EPR, and resonance Raman spectra as the wild-type protein, there is a strong possibility that the axial ligand

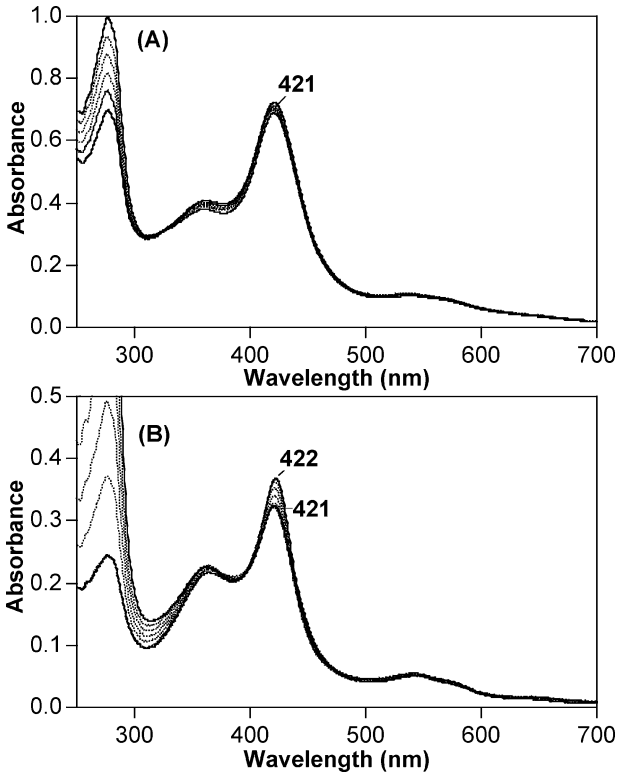

FIGURE 11: Spectra of Fe(III)-bound PAS-A-mPer2 (4 μM) in the presence of various amounts (4, 8, 12, 16, and 20 μM) of heme-free bHLH-PAS-A-NPAS2 (A) and Fe(III)-bound bHLH-PAS-A-NPAS2 (4 μM) in the presence of various amounts (4, 8, 12, 16, and 20 μM) of heme-free PAS-A-mPer2 (B). Spectral changes were observed for (B) but not for (A).

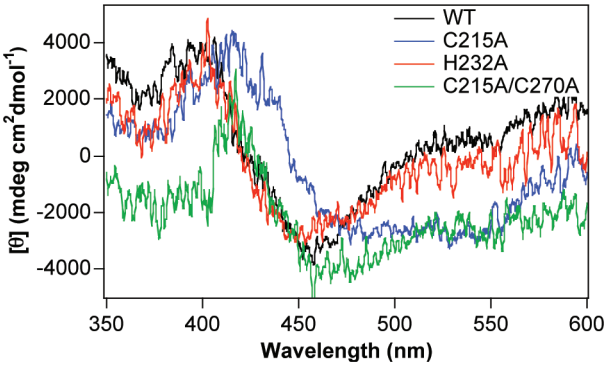

FIGURE 12: CD spectra of the Fe(III) complexes (10 μM) of the wild-type (black), C215A (blue), C215A/C270A (green), and H232A (red) mutant PAS-A-mPer2 proteins. The C215A spectrum was markedly different from that of the wild-type protein. Spectra of other mutant proteins are shown in Figures 3S and 4S (Supporting Infomation). Note that rotational strengths of Fe(III) hemin-bound PAS-A-mPer2 proteins were very low compared with those of other hemoproteins such as myoglobin, hemoglobin, and HRI, thus giving rise to noisy CD spectra.

trans to Cys is hydroxide or water. The optical absorption spectrum of the Fe(III) complex of PAS-A-mPer2 did not alter between pH 7 and pH 10, suggesting that even at pH 7 hydroxide ion (but not water) is the axial ligand *trans* to Cys and gives rise to the low-spin complex.

Heme movement was specifically observed from heme-bound bHLH-PAS-A-NPAS2 to heme-free PAS-A-mPer2. Since association rate constants are obtained by mixing the Fe(II)−CO complex with protein, no significant differences in the dissociation rate constant among heme proteins were evident at a k_{on} value of around 10^7 M^{-1} s^{-1} (Table 3). Thus, the capability of the heme shuttle rate is governed by k_{off} rate constants. The heme dissociation rate constant from bHLH-PAS-A-NPAS2 is higher than that from PAS-A-mPer2 (Table 3), and the apparent dissociation equilibrium constant (1.8×10^{-11} M) for PAS-A-mPer2 is one-tenth (1.6×10^{-10} M) for bHLH-PAS-A-NPAS2. Therefore, heme shuttle from bHLH-PAS-A-NPAS2 to PAS-A-mPer2 observed in the present study appears reasonable. The theory that heme shuttles between NPAS2 and mPer2 (*15*) was corroborated using purified proteins in the present work.

The heme-binding kinetics of the Cys mutants of PAS-A-mPer2 were the same as those of the wild-type protein. Mutations at the heme axial ligands of the other heme-sensor protein, HRI, also did not change its heme-binding characters (our unpublished observations). Global protein folding or hydrophobic interactions between the heme plane and the protein surface due to heme iron coordination would be critical for heme recognition or heme sensing of heme-sensor proteins rather than merely heme coordination, as shown by the results of the axial ligand mutants of the isolated heme-binding subdomain.

The stretching frequency parameters of the resonance Raman spectra of the Fe(II) complexes of the heme-PAS proteins (mPer2, NPAS2, *Ec* DOS) are located at the central region (*12*), suggesting there is no specific ionic interaction of CO bound to the Fe(II) complex. Thus, the interaction between the distal amino acid(s) with bound CO and the Fe(II) complex may not be as strong as those observed for myoglobin, CooA, and sGC (*12*). However, the Fe(II) complexes of NPAS2 and *Ec* DOS have a bis-His or Met-His structure, respectively (*9, 10, 12, 21*), suggesting that CO bound to the Fe(II) complex is located in a polar environment. This inconsistency is probably due to the flexibility of the PAS structure of the heme-sensor protein, so that ligand switching easily occurs for axial-ligand mutant proteins.

Site-directed mutagenesis of the heme axial ligand of heme-sensor proteins does not always result in the expected spectral changes. A residue in close proximity to the native axial ligand may switch to coordinate to the heme iron, even in mutant proteins, thus hampering unequivocal identification of the heme axial ligand. This may be caused by protein flexibility of the heme-sensor protein, which is critical for heme sensing. Thus, ligand switching may occur between Cys215 and Cys270 in PAS-A-mPer2. Nevertheless, particular spectroscopic methods, such as CD spectroscopy, have been useful in determining the heme axial ligand (*31, 33–35*). The origin of the Soret CD band was rationalized by theoretical calculations on the heme rotational strengths in myoglobin and hemoglobin, in that interactions between the heme and aromatic groups in close proximity largely contribute to the Soret CD band (*34, 35*). In the present study, the Soret CD band of the C215A mutant protein was markedly different from that of the wild-type protein. The optical absorption, EPR, and resonance Raman spectra of the C215A/C270A double mutant were also different from those of the wild-type protein. The double mutations at both the Cys215 and Cys270 residues substantially changed the protein structure of the heme environment, leading to a different coordination structure due to the loss of Cys ligands. A similar spectral finding was observed for a heme-sensor enzyme, Irr, in that the Soret absorption spectrum of the

Fe(II) complex of Irr changed only after the mutation of three His residues but not by single mutations at the same sites (*39*). The heme-binding characteristics of the heme-transfer proteins HasA and SiaA also appear to be similar to those of the heme-sensor proteins (*40, 41*).

Figure 1 depicts the amino acid sequences of the heme-binding sites of the PAS domains of NPAS2 and the gas-responsive heme-sensor proteins, *Ec* DOS and FixL. Cys215 of mPer2 is close to the putative heme axial ligand, His119, of NPAS2. His232 and His238 of mPer2 are located in the heme axial ligand regions for *Ec* DOS (His77) and FixL (His194). Cys270 may correspond to Cys170 or His171 of NPAS2. Moreover, specific involvement of Cys270 in the heme surrounding structure should not be excluded, since the double mutant C215A/C270A provided spectra different from those of the wild-type protein. Further studies are required to unequivocally identify the axial ligand *trans* to Cys215.

Cys is the axial ligand of bHLH-PAS-A-NPAS2. The heme dissociation rate is rapid, comparable to that of HRI, but significantly higher than that of metmyoglobin (Table 3). Therefore, NPAS2 may also be a heme-responsive heme-sensor protein. Notably, the physicochemical characteristics of PAS-A-mPer2, HRI, and bHLH-PAS-A-NPAS2, including Cys coordination, redox-dependent ligand switching, and rapid heme dissociation rate constant, are similar.

Summary. Data from the present investigation suggest that (i) PAS-A-mPer2 is able to bind the Fe(III) complex with a stoichiometry of 1:1, (ii) Cys215 is the axial ligand for the Fe(III) complex, (iii) redox-dependent ligand switching from Cys to another amino acid occurs when the Fe(III) complex is reduced to the Fe(II) complex, (iv) the heme dissociation rate constant from PAS-A-mPer2 is significantly higher than that from metmyoglobin, and (v) heme iron moves from bHLH-PAS-A-NPAS2 to PAS-A-mPer2. These physicochemical characteristics suggest that mPer2 is a heme-sensor protein. Our data are in agreement with the proposal that heme association/dissociation from NPAS2 with the aid of mPer2 regulates transcription associated with circadian rhythms (*15*).

ACKNOWLEDGMENT

We are grateful to Dr. Atsunari Tanaka for valuable discussions. We thank Drs. Shunsuke Kuwahara and Fumi Nagatsugi for allowing access to their CD spectrometer. We acknowledge Dr. John S. Olson (Rice University) for kindly providing the expression plasmid for H64Y/V68F apomyoglobin. We are also grateful to Dr. Benfang Lei (Montana State University) for valuable discussions about heme transfer.

SUPPORTING INFORMATION AVAILABLE

Oligonucleotides used to generate mutant PAS-A-mPer2 constructs, association of the Fe(III) complex to apoPAS-A-mPer2, Fe(III) complex transfer from holoNPAS2 to apoPAS-A-mPer2, and Soret CD bands of wild-type, H214A, C215A, H238A, C270A, H277A, H278A, and H316A proteins. This material is available free of charge via the Internet at http://pubs.acs.org.

REFERENCES

1. Hunt, T., and Sassone-Corsi, P. (2007) Riding tandem: Circadian clocks and the cell cycle. *Cell 129*, 461–464.
2. Mignot, E., and Takahashi, J. S. (2007) A circadian sleep disorder reveals a complex clock. *Cell 128*, 22–23.
3. Gatfield, D., and Schibler, U. (2007) Proteosomes keep the circadian clock ticking. *Science 316*, 1135–1136.
4. Chen, Z., Odstrcil, E. A., Tu, B. P., and McKnight, S. L. (2007) Restriction of DNA replication to the reductive phase of the metabolic cycle protects genome integrity. *Science 316*, 1916–1919.
5. Liu, A. C., Lewis, W. G., and Kay, S. A. (2007) Mammalian circadian signaling networks and therapeutic targets. *Nat. Chem. Biol. 3*, 630–639.
6. Rutter, J., Reick, M., Wu, L. C., and McKnight, S. L. (2001) Regulation of clock and NPAS2 DNA binding by the redox state of NAD cofactors. *Science 293*, 510–514.
7. Reick, M., Garcia, J. A., Dudley, C., and McKnight, S. L. (2001) NPAS2: An analog of Clock operative in the mammalian forebrain. *Science 293*, 506–509.
8. Dioum, E. M., Rutter, J., Tuckerman, J. R., Gonzalez, G., Gilles-Gonzalez, M. A., and McKnight, S. L. (2002) NPAS2: A gas-responsive transcription factor. *Science 298*, 2385–2339.
9. Mukaiyama, Y., Uchida, T., Sato, E., Sasaki, A., Sato, Y., Igarashi, J., Kurokawa, H., Sagami, I., Kitagawa, T., and Shimizu, T. (2006) Spectroscopic and DNA-binding characterization of the isolated heme-bound basic helix-loop-helix-PAS-A domain of neuronal PAS protein 2 (NPAS2), a transcription activator protein associated with circadian rhythms. *FEBS J. 273*, 2528–2539.
10. Uchida, T., Sato, E., Sato, A., Sagami, I., Shimizu, T., and Kitagawa, T. (2005) CO-dependent activity controlling mechanism of heme-containing CO-sensor protein, NPAS2. *J. Biol. Chem. 280*, 21358–21368.
11. Gilles-Gonzalez, M. A., and Gonzalez, G. (2005) Heme-based sensors: Defining characteristics, recent developments, and regulatory hypothesis. *J. Inorg. Biochem. 99*, 1–22.
12. Uchida, T., and Kitagawa, T. (2005) Mechanism for transduction of the ligand-binding signal in heme-based gas sensory proteins revealed by resonance Raman spectroscopy. *Acc. Chem. Res. 38*, 662–670.
13. Igarashi, J., Kitanishi, K., Martinkova, M., Murase, M., Iizuka, A., and Shimizu, T. (2008) The role of thiolate-heme proteins, other than the P450 cytochromes, in regulation of heme-sensor proteins. *Acta Chim. Slov. 55*, 67–74.
14. Igarashi, J., Sato, A., Kitagawa, T., Yoshimura, T., Yamauchi, S., Sagami, I., and Shimizu, T. (2004) Activation of heme-regulated eukaryotic initiation factor 2α kinase by nitric oxide is induced by the formation of a five-coordinate NO-heme complex: Optical absorption, electron spin resonance, and resonance Raman spectral studies. *J. Biol. Chem. 279*, 15752–15762.
15. Kaasik, K., and Lee, C. C. (2004) Reciprocal regulation of haem biosynthesis and the circadian clock in mammals. *Nature 430*, 467–470.
16. Amezcua, C. A., Harper, S. M., Rutter, J., and Gardner, K. K. (2002) Structure and interactions of PAS kinase N-terminal PAS domain: Model for intramolecular kinase regulation. *Structure 10*, 1349–1361.
17. Erbel, P. J. A., Card, P. B., Karakuzu, O., Bruick, R. K., and Gardner, K. H. (2003) Structural basis for PAS domain hetero dimerization in the basic helix-loop-helix-PAS transcription factor hypoxia-inducible factor. *Proc. Natl. Acad. Sci. U.S.A. 100*, 15504–15509.
18. Vreede, J., van der Horst, M. A., Hellingwerf, K. J., Crielaard, W., and Aalten, D. M. F. (2003) PAS domains. Common structure and common flexibility. *J. Biol. Chem. 278*, 18434–18439.
19. Zoltowski, B. D., Schwerdtfeger, C., Widom, J., Loros, J. J., Bilwes, A. M., Dunlap, J. C., and Craine, B. R. (2007) Conformational switching in the fungal light sensor vivid. *Science 316*, 1054–1057.
20. Halavaty, A. S., and Moffat, K. (2007) N- and C-terminal flanking regions modulate light-induced signal transduction in the LOV2 domain of the blue light sensor phototropin 1 from *Avena sativa*. *Biochemistry 46*, 14001–14009.
21. Kurokawa, H., Lee, D. S., Watanabe, M., Sagami, I., Mikami, B., Raman, C. S., and Shimizu, T. (2004) A redox-controlled molecular switch revealed by the crystal structure of a bacterial heme PAS sensor. *J. Biol. Chem. 279*, 20186–20193.
22. Sasakura, Y., Yoshimura-Suzuki, T., Kurokawa, H., and Shimizu, T. (2006) Structure-function relationships of *Ec*DOS, a heme-regulated phosphodiesterase from *Escherichia coli*. *Acc. Chem. Res. 39*, 37–43.
23. Hargrove, M. S., Barrick, D., and Olson, J. S. (1996) The association rate constants for heme binding to globin is independent of protein structure. *Biochemistry 35*, 11293–11299.

24. Hargrove, M. S., Singleton, E. W., Quillin, M. L., Ortiz, L. A., Jr., Olson, J. S., and Mathews, A. J. (1994) His64(E7)-Tyr apomyoglobin as a reagent for measuring rates of hemin dissociation. *J. Biol. Chem. 269*, 4207–4214.
25. Dawson, J. H., Andersson, L. A., and Sono, M. (1982) Spectroscopic investigations of ferric cytochrome P-450-CAM ligand complexes: Identification of the ligand trans to cysteinate in the native enzyme. *J. Biol. Chem. 257*, 3606–3617.
26. Sono, M., Roach, M. P., Coulter, E. D., and Dawson, J. H. (1996) Heme-containing oxygenases. *Chem. Rev. 96*, 2841–2888.
27. Martinkova, M., Igarashi, J., and Shimizu, T. (2007) Eukaryotic initiation factor 2α kinase is a nitric oxide-responsive mercury sensor enzyme: Potent inhibition of catalysis by the mercury cation and reversal by nitric oxide. *FEBS Lett. 581*, 4109–4114.
28. Miksanova, M., Igarashi, J., Minami, M., Sagami, I., Yamauchi, S., Kurokawa, H., and Shimizu, T. (2006) Characterization of heme-regulated eIF2α kinase: Roles of the N-terminal domain in the oligomeric state, heme binding, catalysis, and inhibition. *Biochemistry 45*, 9894–9905.
29. Spiro, T. G., and Li, X.-Y. (1988) in *Biological Applications of Raman Spectroscopy* (Spiro, T. G., Ed.) Vol. 3, pp 1−37, John Wiley & Sons, New York.
30. Sato, E., Sagami, I., Uchida, T., Sato, A., Kitagawa, T., Igarashi, J., and Shimizu, T. (2004) SOUL in mouse eyes is a new hexametric heme-binding protein with characteristic optical absorption, resonance Raman spectral, and heme-bonding properties. *Biochemistry 43*, 14189–14198.
31. Inuzuka, T., Yun, B. G., Ishikawa, H., Takahashi, S., Hori, H., Matts, R. L., Ishimori, K., and Morishima, I. (2004) Identification of crucial histidines for heme binding to the N-terminal domain of the heme-regulated eIF2α kinase. *J. Biol. Chem. 279*, 6778–6782.
32. Ishikawa, H., Kato, M., Hori, H., Ishimori, K., Krisato, T., Tokunaga, F., and Iwai, K. (2005) Involvement of heme regulatory motif in heme-mediated ubiquitination and degradation of IRP2. *Mol. Cell 19*, 171–181.
33. Hirata, S., Matsui, T., Sasakura, Y., Sugiyama, S., Yoshimura, T., Sagami, I., and Shimizu, T. (2003) Characterization of Met95 mutants of a heme-regulated phosphodiesterase from *Escherichia coli*: Optical absorption, magnetic circular dichroism, circular dichroism, and redox potentials. *Eur. J. Biochem. 270*, 4771–4779.
34. Hsu, M. C., and Woody, R. W. (1971) The origin of the heme Cotton effects in myoglobin and hemoglobin. *J. Am. Chem. Soc. 93*, 3515–3525.
35. Kiefl, C., Screerama, N., Haddad, R., Sun, L., Jentzen, W., Lu, Y., Qiu, Y., Shelnutt, J. A., and Woody, R. W. (2002) Heme distortions in sperm-whale carbonmonoxy myoglobin: Correlations between rotational strengths and heme distortions in MD-generated structures. *J. Am. Chem. Soc. 124*, 3385–3394.
36. Shimizu, T., Hikage, N., Kitanishi, K., Murase, M., Iizuka, A., Ishikawa, S., Ishitsuka, K. Saiful, I., Yamauchi, S., Tanaka, A., Martinkova, M., Igarashi, J., and Sagami, I. (2007) Structure-function relationships of the thiol-coordinated heme proteins, HRI, associated with protein synthesis, and NPAS2, a regulator of circadian rhythms, Proceeding of the 15th International Conference on Cytochromes P450—Biochemistry, Biophysics and Functional Genomics (Bled, Slovenia, June 17−21), Medmond, International Proceedings, Bologna, Italy.
37. Ran, Y., Zhu, H., Liu, M., Fabian, M., Olson, J. S., Aranda, R., IV, Phillips, G. N., Dooley, D. M., and Lei, B. (2007) Bis-methionine ligation to heme iron in the streptococcal cell surface protein shp facilitates rapid hemin transfer to HtsA of the HtsABC transporter. *J. Biol. Chem. 282*, 31380–31388.
38. de Villiers, K. A., Kaschula, C. H., Egan, T. J., and Marques, H. M. (2007) Speciation and structure of ferriprotoporphyrin IX in aqueous solution: spectroscopic and diffusion measurements demonstrate dimerization, but not μ-oxo dimer formation. *J. Biol. Inorg. Chem. 12*, 101–117.
39. Yang, J., Ishimori, K., and O'Brian, M. R. (2005) Two heme binding sites are involved in the regulated degradation of the bacterial iron response regulator (Irr) protein. *J. Biol. Chem. 280*, 7671–7676.
40. Lukat-Rodgers, G., Rodgers, K. R., Caillet-Saguy, C., Izadi-Pruneyre, N., and Lecroisey, A. (2008) New heme ligand displacement by CO in the soluble hemophore HasA and its proximal ligand mutants: Implication for heme uptake and release. *Biochemistry 47*, 2678–2688.
41. Sook, B. R., Block, D. R., Sumithran, S., Montañez, G. E., Rogers, K. R., Dawson, J. H., Eichenbaum, Z., and Dixon, D. W. (2008) Characterization of SiaA, a streptococcal heme-binding protein associated with a heme ABC transport system. *Biochemistry 47*, 2678–2688.
42. Liu, M., Tanaka, W. T., Zhu, H., Xie, G., Dooley, D. M., and Lei, B. (2008) Direct hemin transfer from IsdA to IsdC in the iron-regulated surface determinant (Isd) heme acquisition system at *Staphylococcus aureus*. *J. Biol. Chem. 283*, 6668–6676.

BI7023892